

Connexin43 knockdown or overexpression modulates cell coupling in control and failing rabbit left ventricular myocytes

Xun Ai*, Weiwei Zhao, and Steven M. Pogwizd

Division of Cardiovascular Disease, Department of Medicine, UAB Center for Cardiovascular Biology, UAB Center for Aging, University of Alabama at Birmingham, 1670 University Boulevard, Volker Hall B140, Birmingham, AL 35294, USA

Received 7 August 2009; revised 22 October 2009; accepted 27 October 2009; online publish-ahead-of-print 30 October 2009

Time for primary review: 48 days

Aims

We have shown that failing human and rabbit left ventricle (LV) exhibits downregulation and dephosphorylation of connexin43 (Cx43) and that Cx43 dephosphorylation in heart failure (HF) contributes to reduced cell coupling. However, the role of Cx43 downregulation *per se* in impaired coupling in HF is unclear.

Methods and results

First, we used adenovirus (Ad) encoding a Cx43 siRNA sequence to knock down Cx43 protein levels in cultured control rabbit LV myocytes. Cells cultured for up to 48 h with intermittent pacing maintained Cx43 protein levels and phosphorylation status. Cell coupling in Cx43 knockdown myocyte pairs (by Lucifer Yellow dye transfer) was markedly reduced after 24 h infection (associated with ~40% Cx43 knockdown) and after 48 h (associated with ~70% Cx43 knockdown). The phosphorylation status, distribution of remaining Cx43 proteins, and levels of other cardiac connexins (Cx40 and Cx45) were unchanged. Second, we overexpressed Cx43 to levels comparable to control using an adenovirus encoding wild-type Cx43 (Cx43WT) gene in isolated LV myocytes from our arrhythmogenic HF rabbit model. We found 87% more Cx43WT proteins improved dye coupling [vs. Ad- β -galactosidase (LacZ) infected HF controls]. Overexpressed Cx43 protein was located throughout the myocyte membrane (same pattern as in controls), and the phosphorylation status of Cx43 remained comparable to that in AdLacZ infected HF controls.

Conclusion

In addition to Cx43 dephosphorylation, downregulation of Cx43 plays an essential role in reduced cell coupling in the failing rabbit heart. Modulation of Cx43 expression could be a novel therapeutic approach to improve conduction and decrease sudden death in HF.

Keywords

Connexin43 • Protein expression • Intercellular coupling • Heart failure • Arrhythmia

1. Introduction

Nearly 5 million Americans are suffering from heart failure (HF).¹ Deaths in patients with HF (whether due to non-ischaemic or ischaemic HF) occur suddenly in nearly one half of patients, primarily from ventricular tachycardia (VT) degenerating to ventricular fibrillation (VF).¹ However, effective pharmacological approaches to prevent the development of these lethal arrhythmias in HF remains limited due to our lack of understanding of the underlying electrophysiological and biochemical mechanisms.

VT in non-ischaemic HF initiates primarily by a non-reentrant mechanism.² However, myocardium from patients with non-ischaemic HF due to idiopathic dilated cardiomyopathy exhibits non-uniform anisotropy, slow conduction, and conduction block³ that could underlie reentry during the transition from VT to VF. There is accumulating evidence that alterations in intercellular coupling involving cardiac gap junctions may underlie slow conduction in non-ischaemic HF. We⁴ and others^{5,6} have shown that ~40% reduction of connexin43 (Cx43) [mRNA and protein in both left ventricle (LV) tissue and isolated LV myocytes] was

* Corresponding author. Tel: +1 205 934 1361, Fax: +1 205 934 1268, Email: xai@uab.edu

associated with decreased intercellular coupling and, ultimately, slow conduction in the failing human heart and experimental HF animal models. Moreover, we reported for the first time that with HF there is an enhanced dephosphorylation of Cx43 which is due to an increased level of protein phosphatase 2A (PP2A) that is co-localized with Cx43 protein. This increased dephosphorylation of Cx43 leads to impaired intercellular coupling, evident by improvement in intercellular coupling with protein phosphatase inhibition.⁴ However, the functional role of downregulated Cx43 expression *per se* in impaired intercellular coupling in HF is not well understood.

Although a number of agents have been used to block gap junction channels to study the functional role of gap junction channels in isolated myocytes or perfused animal heart,⁷ those agents can also block other ion channels (such as Na channels)⁸ and can even change intracellular pH.⁹ Therefore, genetically engineered mice that lack Cx43 proteins had been generated to define the role of Cx43 expression in conduction. While homogenous Cx43 knockout mice are embryologically lethal,¹⁰ Cx43 heterozygous knockout mice (with a 50% reduction of Cx43 protein vs. wild-type mice) have a normal lifespan. However, the results of cardiac electrophysiological abnormalities from Cx43 knockdown hearts have been conflicting, with slow ventricular conduction noted in some studies,^{10,11} but normal conduction observed in others.¹² A recently developed transgenic mouse model with cardiac specific Cx43 ablation during development¹³ showed slowed conduction when Cx43 was reduced up to 80%, but unchanged conduction when 40% of Cx43 was deleted (although there was a trend toward slow conduction). Overall, these results raise questions as to whether a ~40–50% downregulation of Cx43 proteins (such as in HF) can affect intercellular coupling significantly. It is well known that Cx43 is a phosphoprotein and that the phosphorylation state of Cx43 plays an important role in intercellular coupling.¹⁴ As such, the unknown phosphorylation state of the remaining 50% Cx43 in the Cx43^{-/+} transgenic mouse hearts in these studies could contribute to the disparate results.

Thus, to explore the role of Cx43 protein expression in modulating coupling, we knocked down Cx43 protein by a novel small interfering RNA (siRNA) gene silencing approach in cultured adult control rabbit myocytes. Then, to further define the role of downregulated Cx43 in HF myocytes, we overexpressed Cx43 in isolated LV myocytes from HF rabbits using an adenovirus (Ad) encoding a wild-type rat Cx43 gene sequence. Intercellular coupling was assessed using our well-developed Lucifer Yellow (LY) dye microinjection technique⁴ in isolated cardiac myocyte pairs. The phosphorylation state and distribution of Cx43 proteins were also determined using immunocytochemistry and immunoblotting approaches. Our studies provide further evidence that Cx43 protein levels (independent of Cx43 phosphorylation and distribution) modulate intercellular coupling in heart and that Cx43 downregulation in HF *per se* contributes to intercellular uncoupling.

2. Methods

An expanded Materials and Methods section is available as Supplementary material online.

2.1 Generating and purifying recombinant adenoviruses

Recombinant adenoviruses containing specific pre-designed siRNA sequences including Cx43 (Cx43siRNA), GAPDH (GAPDHsiRNA, positive control), and scrambled negative (adNegsiRNA, negative control) were constructed according to the manufacturer's instruction (Ambion). Adenoviruses encoding the full length of wild-type rat Cx43 DNA (AdCx43WT) and LacZ (AdLacZ) were obtained as gifts from Dr Eric Beyer (University of Chicago).

2.2 Obtaining LV tissue and isolated myocyte from control and failing rabbit heart

New Zealand White rabbits underwent induction of HF as previously described.^{2,4} The LV tissue and isolated myocytes were obtained from HF and age-matched control rabbits. The investigation conforms with the Guide for the Care and Use of Laboratory Animals published by the US National Institutes of Health (NIH Publication No.85-53, revised 1996). The protocol was also approved by the UIC Animal Studies Committee (No: 04-117) and the University of Alabama at Birmingham Institutional Animal Care and Use Committee (No: 090208356).

2.3 Adenoviral infection in isolated LV myocytes from control and HF rabbits

Isolated LV myocytes from control and HF rabbits were infected with AdCx43siRNA (or with AdGAPDHsiRNA or AdNegsiRNA as controls) or AdCx43WT (with AdLacZ as a negative control), then cultured with pacing in a supplemented M199 medium for up to 48 h. Adenoviral infection efficacy was determined by assessing β -galactosidase expression using X-Gal staining.

2.4 Western blot analysis and PCR

Western blotting was performed as previously described.⁴ Total Cx43 protein (Cx43-T) was assessed using a polyclonal Cx43-T antibody (Zymed). The non-phosphorylated isoform of Cx43 (Cx43-NP) was detected by a specific monoclonal Cx43-NP antibody (Zymed).⁴ Total RNA was isolated using TRIzol reagent (Gibco). RT-PCR was performed using One-step hot-start RT-PCR kit (Invitrogen).

2.5 Immunofocal microscopy

Immunostaining was carried out with polyclonal Cx43-T, monoclonal Cx43-NP antibodies (as above), and N-cadherin antibody (Zymed). Images were collected from a laser scanning confocal microscope (Carl Zeiss).

2.6 Microinjection of LY

Four percent LY combined with 1% Rhodamine B dextran was microinjected into one cell of each cell pair in M199 cell culture medium; microinjection and image recording were then performed under a confocal microscope (Carl Zeiss), and intercellular coupling was assessed as previously described.⁴

2.7 Statistical analysis

All data were presented as means \pm SEM. Differences between two groups were evaluated using one-way ANOVA Tukey's Multiple Comparison test, and $P < 0.05$ was considered to be significant.

3. Results

3.1 Development of HF

With HF, LV end-diastolic dimension increased by 49% (1.52 ± 0.02 to 2.27 ± 0.06 cm, $P < 0.0001$), LV end-systolic dimension increased by 79% (0.94 ± 0.03 to 1.69 ± 0.05 cm, $P < 0.0001$), and mean fractional shortening decreased by 33% (38 ± 1 to $25 \pm 1\%$, $P < 0.0001$ vs. baseline).

3.2 Preservation of Cx43 protein content and phosphorylation state in paced culture myocytes

In preparation for Cx43 knockdown studies, we cultured isolated adult rabbit myocytes with or without pacing up to 48 h (Supplementary material online, *Figure S1B* and *C* compared with freshly isolated myocytes (Fresh) in Supplementary material online, *Figure S1A*). Western blots of isolated rabbit LV myocytes using anti-Cx43-T (*Figure 1A*, top) distinguished the lower molecular weight (NP 42 kDa) band, which represents Cx43-NP, from the higher molecular weight (43–46 kDa) bands which represent phosphorylated isoforms of Cx43 (P1 and P2). Culturing control rabbit cardiac myocytes without pacing for 24 or 48 h (C24, C48) led to a significant decrease in total Cx43 expression (*Figure 1A* and *B*, left) that was associated with a marked increase in Cx43-NP (*Figure 1D* and *F*, left) (vs. Fresh). However, pacing cultured rabbit myocytes for 24 or 48 h (P24, P48) preserved Cx43 protein content and phosphorylation state (vs. Fresh; *Figure 1A–D*, right). We also used the specific anti-Cx43-NP antibody to identify Cx43-NP and found similar results (data not shown). Immunostaining results (*Figure 1D*) further confirmed unaltered expression as well as distribution of Cx43 protein in paced cultured myocytes. Therefore, all subsequent cell culture and transduction studies were done with pacing.

3.3 Reduced intercellular dye coupling in Cx43 knockdown rabbit myocytes

We performed siRNA gene silencing experiments with recombinant AdCx43siRNA in control rabbit LV myocytes. X-Gal staining of fixed AdCx43siRNA infected myocytes showed a high efficiency of viral infection, with >99% of the cell population staining positive (*Figure 2A*). After 24 h, AdCx43siRNA knocked down Cx43 protein expression ~40% (comparable to that seen in HF rabbit myocytes)⁴ (*Figure 2B*, third lane and *C*, middle). After 48 h, Cx43 expression was further knocked down by ~70% (*Figure 2B*, fourth lane and *C*, right). Summarized immunoblot data also revealed that the ratio of non-phosphorylated to phosphorylated Cx43 was unchanged (*Figure 2D*). The knockdown of Cx43 mRNA was also confirmed by using RT-PCR technique (data not shown). With Cx43 knockdown, expression of other cardiac connexins (Cx40 and Cx45) remained the same (*Figure 2E* and *F*). We used AdGAPDHsiRNA, a positive control, and found a nearly 60% reduction in GAPDH protein, while the levels of Cx43 protein remained unchanged (*Figure 2B*, second lane). Moreover, AdNegsiRNA, a negative control, had no knockdown effect on either Cx43 or GAPDH protein (*Figure 2B*, first lane). Immunostaining with Cx43-T antibody further confirmed

the marked reduction of Cx43 protein in AdCx43siRNA infected myocytes, and that the distribution of the remaining Cx43 proteins, which co-localized with N-cadherin proteins, was unchanged (*Figure 2G* and *H*). Our results clearly demonstrate the efficacy and specificity of AdCx43siRNA in knocking down Cx43 expression in paced cultured control rabbit LV myocytes.

We then assessed intercellular coupling by LY dye transfer experiments. *Figure 3A* and *B* shows representative sequential confocal images (at 1, 38, and 217 s) following LY microinjection into one cell of AdCx43siRNA and AdCx43siRNA infected control end-to-end cell pairs. Cx43 knockdown myocytes had decreased intercellular coupling (slower dye transfer), with a 97% increase of rate constant (τ , time to reach ~63% peak) at 24 h (70.6 ± 1.2 s) that was associated with ~40% Cx43 knockdown (*Figures 2C*, middle; *3C* and *D*, middle). At 48 h, τ had a 224% increase (116.0 ± 5.7 s) that was associated with ~70% Cx43 knockdown (*Figures 2C*, right; *3C* and *D*, right). These were both significantly different vs. AdNegsiRNA infected controls ($\tau = 35.8 \pm 2.9$ s; *Figure 3C* and *D*, left). These results (summarized in *Figure 3E*) strongly suggest that knockdown of Cx43 (without changing phosphorylation state and distribution of remaining Cx43 protein) in control rabbit myocytes significantly reduces intercellular coupling.

3.4 Downregulated Cx43 expression and unchanged distribution of Cx43 proteins with N-cadherin protein in non-ischaemic HF LV

We have previously shown downregulation of Cx43 at both the mRNA and protein levels in HF.⁴ Here we further determine whether there are alterations in the distribution of Cx43 proteins associated with the anchoring protein N-cadherin in HF by using immunofluorescence staining and confocal microscopy. Paraformaldehyde-fixed and paraffin-embedded LV tissue sections were double-stained with Cx43-T plus Cx43-NP, or Cx43-T plus N-cadherin antibodies, respectively (*Figure 4A–D*). There was no fluorescence signal found by staining with the secondary antibody only (negative controls, data not shown). *Figure 4A* and *B* demonstrates that Cx43 proteins (total and NP) were localized throughout the myocyte membrane in distinctive punctuate patterns, primarily at cell ends (rather than sides) in both control and HF. In HF LV tissue sections (vs. controls), there was less total Cx43 proteins and greater Cx43-NP isoforms (as we previously showed)⁴ that was associated with an unchanged amount of N-cadherin proteins (*Figure 4C* and *D*). In addition, immunoblotting data (*Figure 4E* and *F*) showed that N-cadherin protein expression in HF LV did not differ from control (normalized to GAPDH).

3.5 Overexpression of Cx43 in isolated HF rabbit myocytes

To offset the downregulated Cx43 protein with HF, we overexpressed wild-type Cx43 in isolated HF rabbit LV myocytes by infecting them with AdCx43WT and continually culturing for up to 24 h. Immunoblot data from AdCx43WT infected HF myocytes showed that Cx43-T protein expression (measured as the 42–46kDa band) was increased ~87% (vs. AdLacZ infected HF myocytes; *Figure 5A* and *B*, left). The ratio of non-phosphorylated to

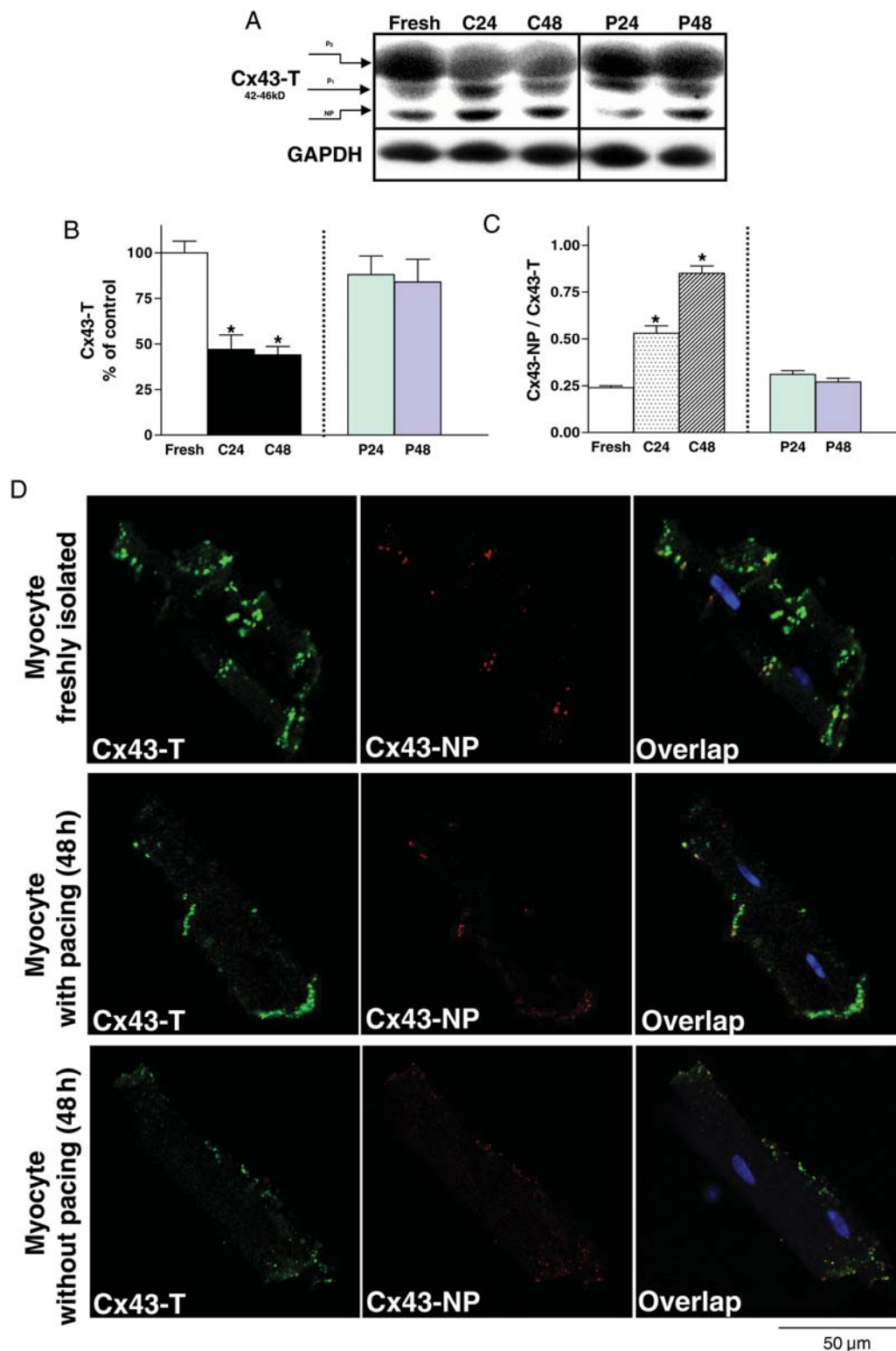


Figure 1 (A) Immunoblot images of total Cx43 (Cx43-T, at top, P₁ and P₂ represent phosphorylated Cx43 isoforms and NP represents non-phosphorylated Cx43 isoform) and GAPDH (bottom) bands. Sequential lanes include freshly isolated control LV myocytes (Fresh, $n = 4$) and myocytes cultured for 24 or 48 h without pacing (C24, C48; $n = 4$) or with pacing (P24, P48; $n = 4$). (B and C) Summarized data for total Cx43 protein (Cx43-T = P₁ + P₂ + NP) expression and for the ratio of Cx43-NP isoform to Cx43-T protein (Cx43-NP/Cx43-T) (* $P < 0.05$). (D) Double immunofluorescence staining with Cx43-T (green, at left) and Cx43-NP (red, middle) antibodies in myocytes from control rabbit LV that were freshly isolated (top) cultured 48 h with pacing (middle) or cultured 48 h without pacing (bottom) (scale bar = 50 μ m). Far right panel is the overlap images along with DAPI (blue, nucleus labelling).

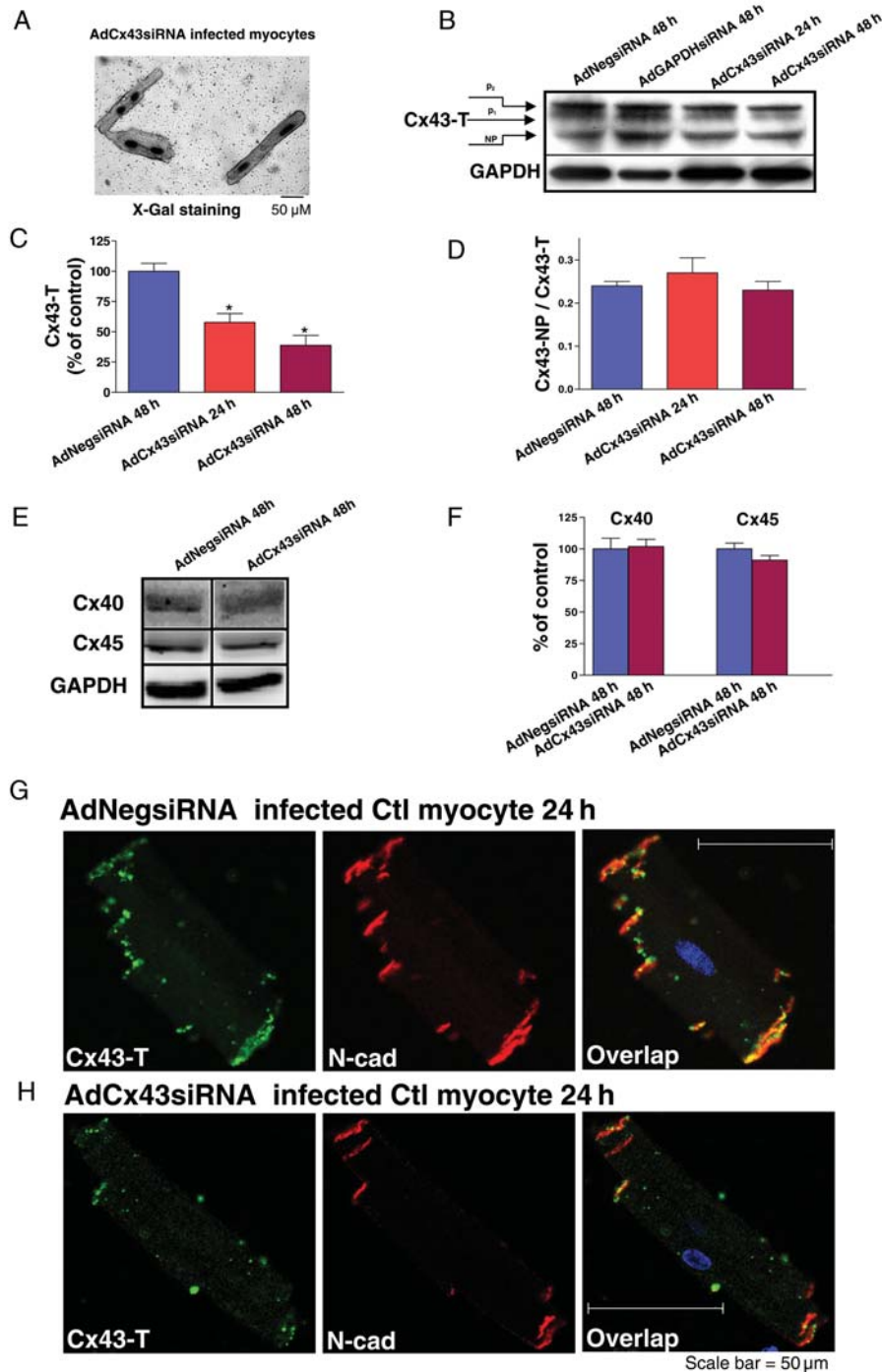


Figure 2 (A) Image of X-Gal staining in AdCx43siRNA infected control myocytes (scale bar = 50 μ m). (B) Immunoblot images of Cx43-T (top) and GAPDH (bottom) bands from AdNegsiRNA infected control adult LV myocytes at 48 h, AdGAPDHsiRNA infected cells at 48 h, and AdCx43siRNA infected cells at 24 and 48 h. (C and D) Summarized data for total Cx43 expression (Cx43-T; $*P < 0.05$, $n = 4$) and the ratio of Cx43-NP isoform to Cx43-T protein (Cx43-NP/Cx43-T; $P = \text{NS}$) from AdCx43siRNA infected cells at 48 h, and for AdCx43siRNA infected cells at 24 or 48 h. (E) Immunoblot images of Cx40 (top), Cx45 (middle), and GAPDH (bottom) from AdCx43siRNA and AdCx43siRNA infected myocytes at 48 h (data were obtained from the same blot). (F) Pooled data for Cx40 and Cx45 protein expression from AdCx43siRNA and AdCx43siRNA infected myocytes at 48 h ($P = \text{NS}$, $n = 3$). Double immunofluorescence staining in control rabbit LV myocytes at 24 h that were infected with AdNegsiRNA (G) or AdCx43siRNA (H) with total Cx43 (Cx43-T, green) and N-cadherin (N-cad, red) antibodies. At far right are the overlap images with Cx43-T and N-cadherin signals (yellow) along with DAPI staining of nuclei (blue).

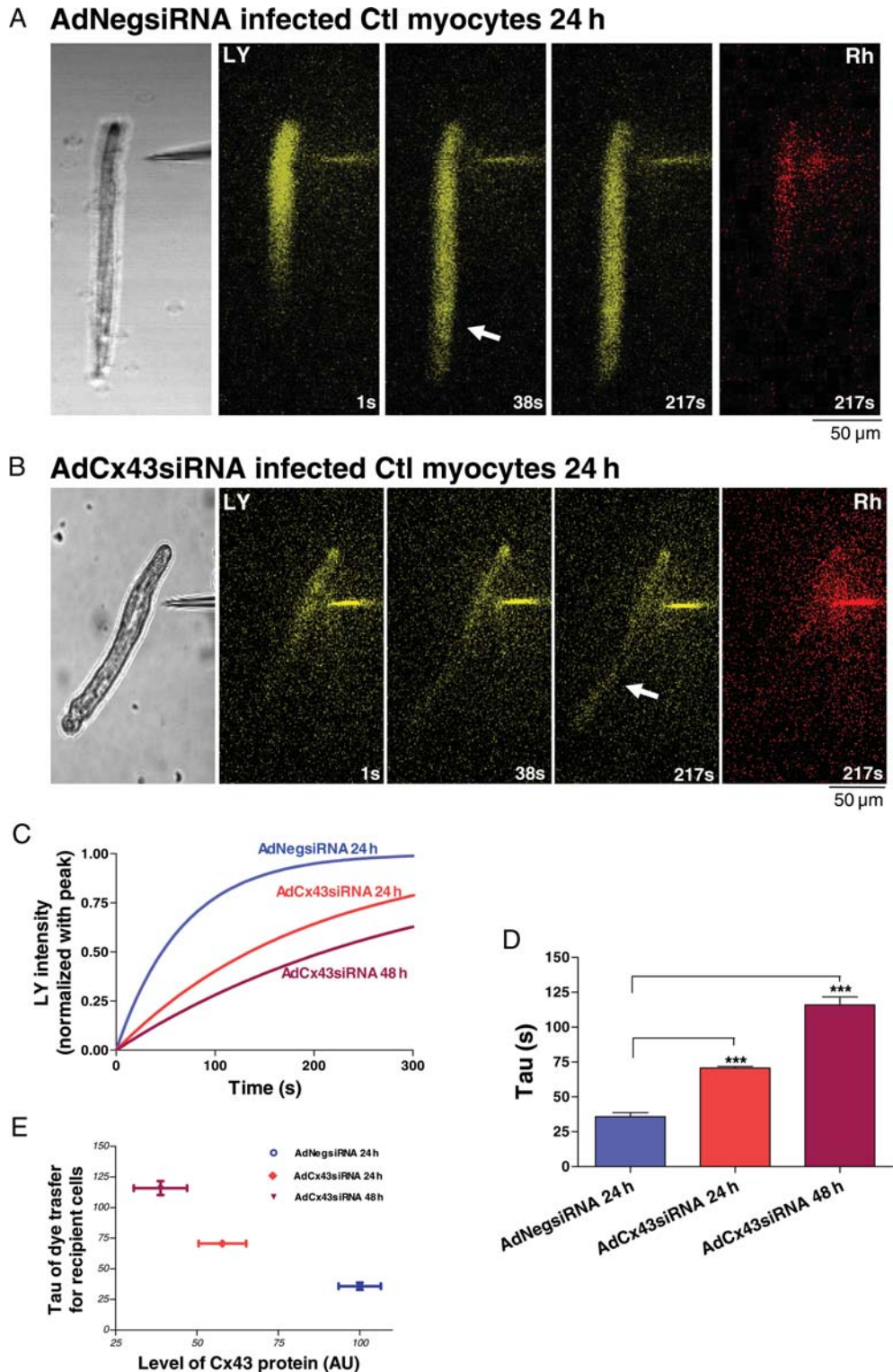


Figure 3 Lucifer Yellow (LY) microinjection images of subsequent LY dye transfer from a single injected cell to the adjacent recipient cell. At left are the phase contrast images in AdNegsiRNA (A) and AdCx43siRNA (B) infected control rabbit LV myocytes. In the middle three panels are sequential dye transfer images at 1, 38, 217 s (yellow). Arrows denote early spread of dye to the non-injected cell of the cell pair, which appears later in AdCx43siRNA infected myocyte pairs. At far right are images of Rhodamine B dextran (Rh, red) retained in the injected myocytes. Scale bar at lower left = 50 μ m. (C) Representative fitted single time courses of LY transfer in recipient cell from control LV end-to-end cell pairs infected with AdNegsiRNA at 24 h and with AdCx43siRNA at 24 and 48 h, respectively. (D) Summarized τ data of LY transfer in recipient cell from AdCx43siRNA infected cells at 24 h and AdCx43siRNA infected myocytes at 24 and 48 h (***) ($P < 0.001$, $n = 3$). (E) Plot of τ as a function of relative Cx43 protein level in AdCx43siRNA infected cells at 24 h and AdCx43siRNA infected myocytes at 24 and 48 h.

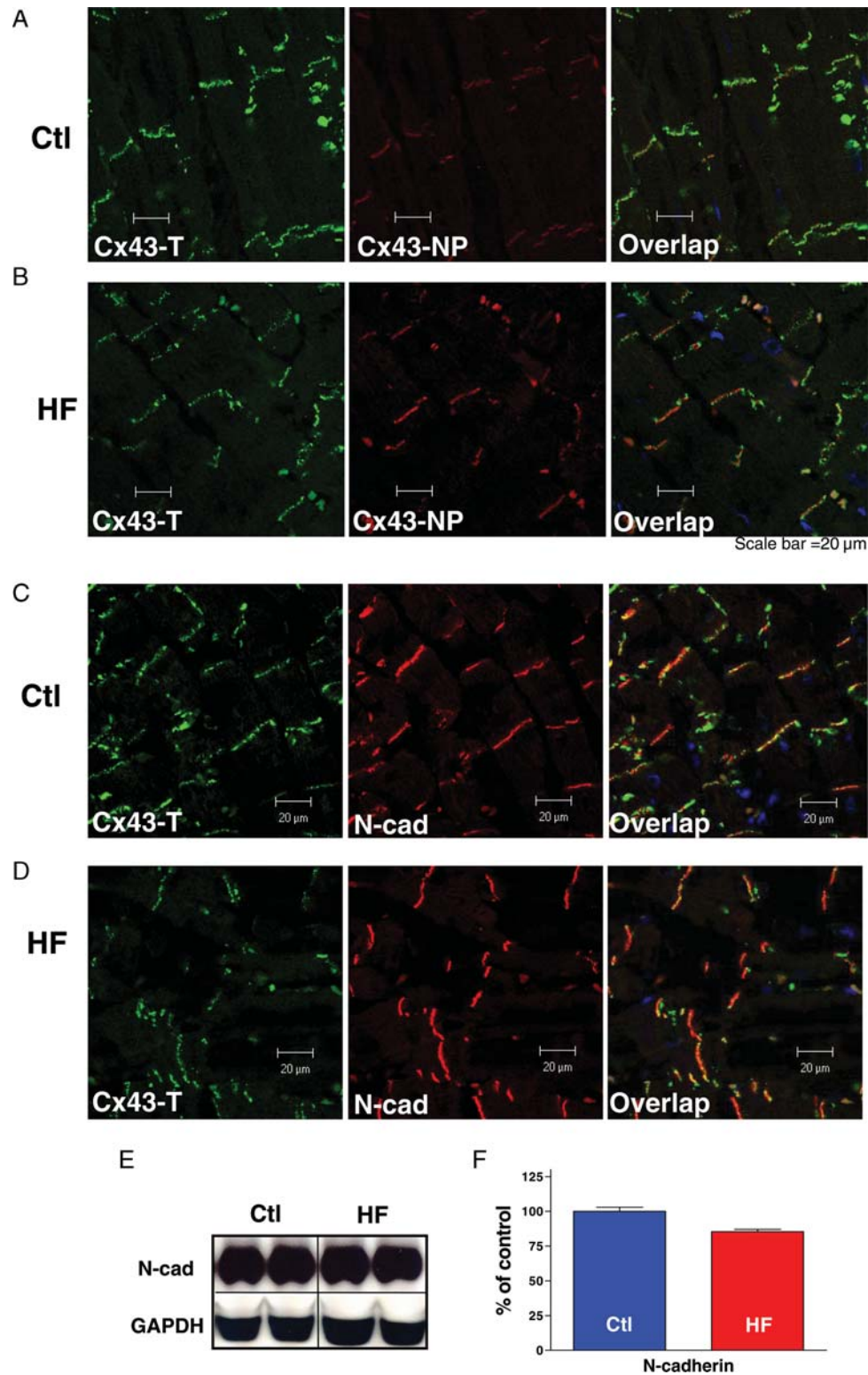


Figure 4 Double immunofluorescence staining of control (A) and HF rabbit (B) LV tissue sections with Cx43-T (left, green) and Cx43-NP (middle, red) antibodies. At right are the overlap images (yellow). Double immunofluorescence staining of control (C) and HF rabbit (D) tissue sections with Cx43-T (left, green) and N-cadherin (middle, red) antibodies and the overlap images (right, yellow). Scale bar = 20 μ m. (E) Western blot images of N-cadherin (N-cad, top) and GAPDH (bottom) from control and HF rabbit LV. (F) Summarized data for N-cadherin protein expression ($P = NS$, $n = 8, 10$).

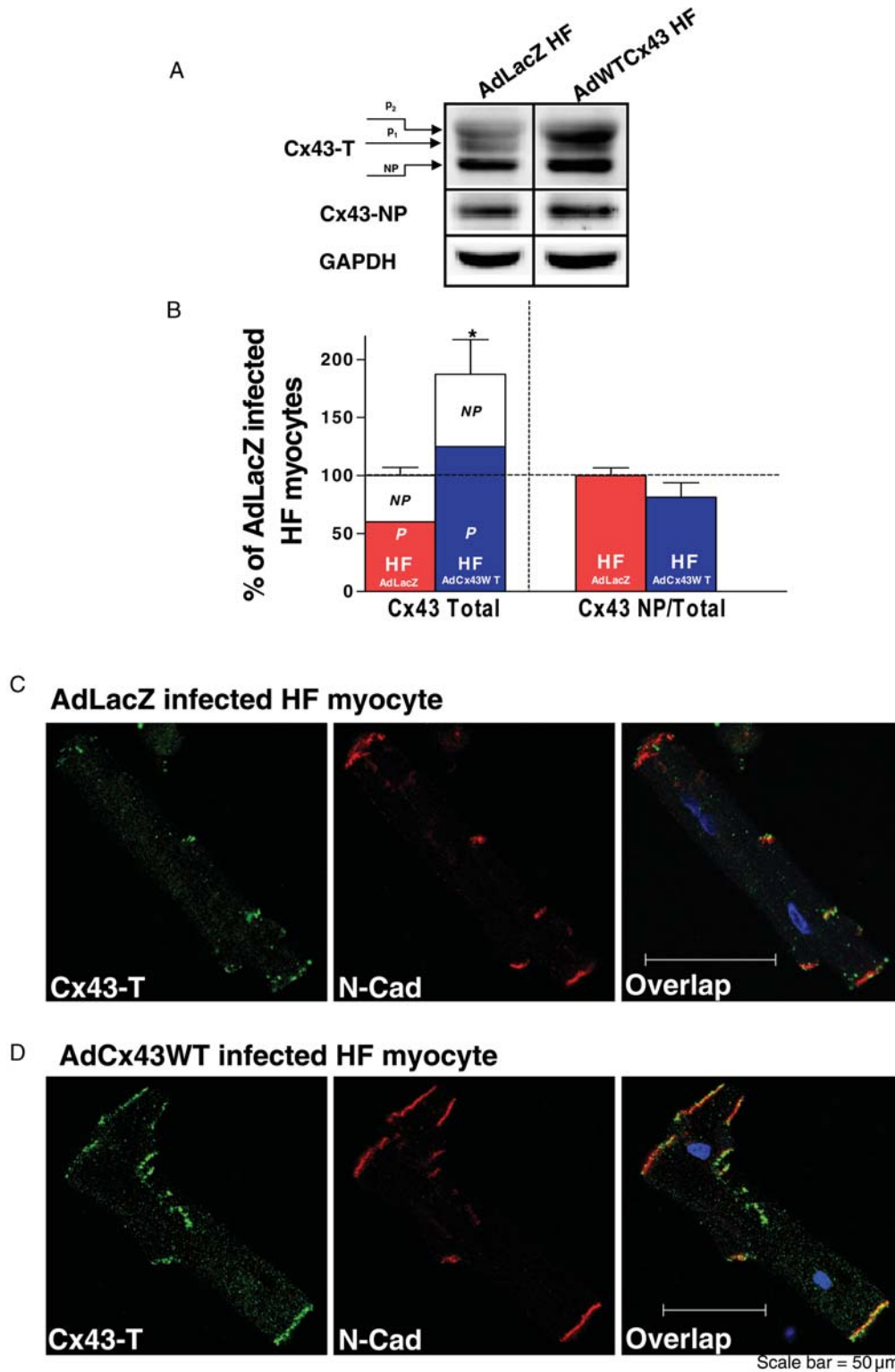


Figure 5 (A) Western blot images of Cx43-T (top), Cx43-NP (middle), and GAPDH (bottom) from AdCx43WT and AdLacZ infected HF myocytes at 24 h (subjected to pacing). (B) Summarized data for Cx43 expression (normalized to GAPDH) in AdCx43WT and AdLacZ infected HF myocytes at 24 h ($*P < 0.05$, $n = 5, 4$). At left are the changes in Cx43-T protein expression with the relative contributions of Cx43-NP (NP) and Cx43-P (P) indicated. At right is the ratio of Cx43-NP (using specific Cx43-NP antibody) to total Cx43 (using Cx43-T antibody). (C and D) Double immunofluorescence staining with Cx43-T (green) and N-cadherin (N-cad, red) antibodies in AdLacZ (C) and AdCx43WT (D) infected HF myocytes after 24 h (with pacing). At far right are overlap images with signals of Cx43-T, N-cadherin, and nuclear staining with DAPI (blue).

total Cx43 in Cx43WT-overexpressed HF myocytes was similar to that in AdLacZ infected HF controls (Figure 5B, far right).

We further assessed the distribution of overexpressed Cx43 proteins in AdCx43WT infected HF myocytes by double immunofluorescence staining with Cx43-T and N-cadherin antibodies using confocal microscopy. Figure 5C and D shows that immunolabelled Cx43-T protein was distributed in a pattern comparable to that in controls. Thus, there was a greater amount of Cx43, but the distribution of overexpressed total Cx43 protein was similar to that in AdLacZ infected HF myocytes.

3.6 Improved intercellular dye coupling in Cx43 overexpressed HF myocytes

To define the effect of overexpressed Cx43 on intercellular coupling in HF myocytes, we performed LY dye transfer experiments as above (Figure 6A and B). We found that AdLacZ infected HF myocytes had an increased dye transfer time ($\tau = 49.9 \pm 1.4$ s; Figure 6C and D), which reflects a decreased intercellular coupling, consistent with our prior findings.⁴ However, AdCx43WT infected HF cell pairs, with a greater amount of Cx43 proteins, and a comparable phosphorylation state and distribution of Cx43 protein compared with HF controls, showed significantly improved dye coupling ($\tau = 15.5 \pm 4.5$ s vs. AdLacZ infected HF controls, Figure 6C and D).

4. Discussion

In our previous study, we found that HF rabbit and human cardiac myocytes exhibit downregulation of Cx43 (mRNA and protein) and enhanced Cx43 dephosphorylation that is associated with decreased intercellular coupling.⁴ Although we reported for the first time that increased amount of PP2A that is co-localized with Cx43 proteins in HF contributed to Cx43 dephosphorylation and, ultimately, intercellular coupling, the role of downregulated Cx43 *per se* in impaired intercellular coupling in HF remains unclear.

In the present study, we showed that knocking down Cx43 proteins by a novel siRNA gene silencing technique in cultured adult control myocytes to a level seen in HF (without changing the distribution and phosphorylation state of the remaining Cx43) resulted in a marked reduction of intercellular dye coupling. We then performed the important complementary studies in which we overexpressed wild-type Cx43 in isolated LV myocytes from HF rabbits using an adenovirus encoding a wild-type rat Cx43 gene sequence. We found a significant improvement in cell dye coupling that was associated with a greater amount of total Cx43 protein (levels comparable to controls) but with no change in the ratio of non-phosphorylated to total Cx43 protein (vs. AdLacZ infected HF myocytes). Our results provide new fundamental evidence that modest reduction of Cx43 protein *per se* contribute to impaired intercellular coupling in the failing heart.

4.1 Preservation of Cx43 protein content and phosphorylation state in paced culture myocytes

It has been reported¹⁵ that culturing adult myocytes for up to 48 h can lead to a substantial reduction in Cx43 protein content and Cx43 redistribution.¹⁵ We cultured isolated adult rabbit myocytes

and found a similar marked reduction in total Cx43 protein content, but also an increase in the dephosphorylated Cx43 isoform. Berger *et al.*¹⁶ had shown that, with regular electrical field stimulation, cultured adult myocytes contracted rhythmically and maintained some of the phenotype and biophysical properties of freshly isolated myocytes. In the present study, we cultured isolated adult rabbit myocytes with a periodic electrical stimulation (0.5 Hz) for up to 48 h and found that Cx43 protein content and phosphorylation state as well as Cx43 distribution were well preserved (comparable to freshly isolated LV myocytes and distinctly different from un-stimulated cultured myocytes). These preserved Cx43 protein properties along with our data of LY dye transfer between myocyte pairs suggest functional gap junction channels were still present in our isolated cultured myocytes. Thus, our results clearly show that electrical field stimulation is a practical approach to maintain not only protein content, but also phosphorylation status and distribution of Cx43 and intact functional gap junctions in cultured adult myocytes.

4.2 The role of reduced levels of Cx43 proteins in intercellular coupling

The role of Cx43 expression *per se* in modulating conduction has been extensively studied in conditional or transgenic Cx43 knockout mouse models.^{10–12,17,18} However, the results of conduction velocity measurements from Cx43 heterozygous mouse hearts (50% reduction of Cx43 protein compared with wild-type mice) have been inconsistent, with some studies showing slowing of conduction,^{10,11} whereas others demonstrated no change.¹² In the present studies, we used a siRNA gene silencing technique to achieve specific and homogeneous knockdown of Cx43 protein in cultured myocytes isolated from control rabbit LV. Our findings of reduced dye coupling in cultured adult myocytes associated with a ~40% or a ~70% knockdown of Cx43 further supports the previous findings of slowing of conduction velocity in Cx43 heterozygous knockout mice heart. In our studies, we excluded the effects of compensation of other cardiac connexin (Cx40 and Cx45) and, more importantly, alterations in distribution and phosphorylation status of the remaining Cx43 protein on reduced cell–cell communication in Cx43 knockdown myocytes.

A recently developed transgenic mouse model with cardiac specific Cx43 ablation during development¹³ showed slow conduction when Cx43 was reduced up to 80%, but unchanged conduction when 40% of Cx43 was deleted. Although studies in an inducible deletion of Cx43 (65–95%) in adult mice (avoiding developmental compensation of Cx43 deficiency, but exhibited myocardial inflammation) showed similar results,¹⁷ it is notable that the phosphorylation status of the remaining Cx43 proteins in these Cx43 deletion transgenic mouse models has not been reported. There are numerous studies showing that the phosphorylation state of Cx43 plays an important role in intercellular coupling.¹⁴ Thus, one cannot exclude that the different results of conduction in Cx43 knockdown mouse hearts and our current results could be due, at least in part, to alterations in the phosphorylation status of remaining Cx43 proteins.

Species differences could also be counted as another important factor. Along these lines, a number of transgenic rabbit models have been shown to exhibit phenotypes that differ considerably

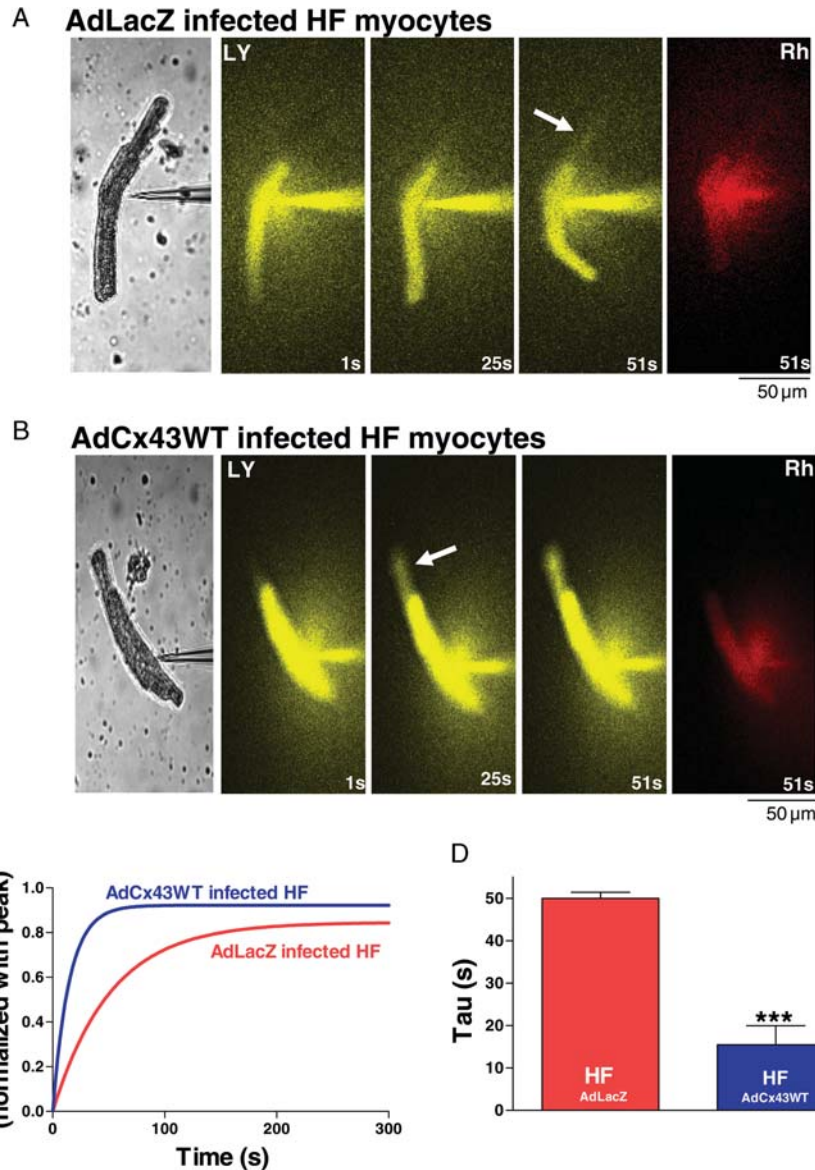


Figure 6 Sequential Lucifer Yellow (LY) dye transfer images (at 1, 25, 51 s) from a single injected cell to a recipient cell in AdLacZ (A) and AdCx43WT infected (B) HF myocyte end-to-end cell pairs at 24 h (phase contrast images are at left panel). Arrows denote early spread of dye to the non-injected cell of the cell pair, which occurs sooner in AdCx43WT infected HF cell pairs. At far right are images of Rhodamine B dextran (Rh, red) retained in the injected myocyte. Scale bar at lower left = 50 μ m. (C) Representative fitted single time courses of LY dye transfer in recipient cell from end-to-end cell pairs of AdLacZ and AdCx43WT infected HF myocytes. (D) Summarized τ data of LY dye transfer in AdLacZ and AdCx43WT infected HF myocytes (** $P < 0.001$, $n = 4, 6$).

from those in transgenic mice^{19,20} For example, transgenic rabbits overexpressing the G protein $G_{s\alpha}$ do not develop cardiomyopathy like their transgenic mouse counterparts;²⁰ and phospholamban overexpressing transgenic rabbits have normal cardiac function and response to β -adrenergic stimulation, unlike the transgenic mouse counterparts.¹⁹ These findings might arise from species differences in compensatory changes and/or species differences in cellular physiology (rabbit calcium handling and ion channel physiology is closer to that of human than what is observed in mouse).²¹ Moreover, there could well be important differences between rodent and rabbit connexins or connexin-associated

proteins that have not been recognized but which could contribute to species-related differences.

4.3 Modulating the amount of Cx43 proteins to improve intercellular coupling in non-ischaemic HF

Although the downregulation of Cx43 seems to be a common feature of the failing heart, the role of downregulated Cx43 *per se* in intercellular coupling in HF remains unclear. We and others had showed that a $\sim 40\%$ reduction of Cx43 in diseased heart is

associated with impaired intercellular coupling.^{4,22} In a recent report, Roell *et al.*²³ demonstrated that transplantation of Cx43-expressing embryonic cardiac myocytes improved electrical coupling in mice with left ventricular infarcts. Kizana *et al.*²⁴ also reported that lentiviral gene transfer of a Cx43 internal loop mutant attenuated coupling in cultured neonatal rat cardiac myocytes. Although these studies provide additional evidence that amount of functional Cx43 proteins contributes directly to intercellular coupling in diseased heart, the Cx43 phosphorylation state was not reported; so one cannot exclude an important effect by Cx43 phosphorylation state alone. Thus the role of Cx43 protein levels in modulating coupling and the contribution of modestly decreased Cx43 downregulation *per se* to decreased coupling in HF (independent of altered Cx43 phosphorylation or distribution) remain to be clarified.

Although there have been studies of Cx43 expression on intercellular coupling in isolated control mouse myocyte pairs,²⁵ our current results are the first demonstration of the role of Cx43 expression alone in HF myocyte pairs and in a large (non-rodent) animal species. In the present studies, our findings from Cx43 knockdown control myocytes are particularly relevant in that we observed a significant decrease in intercellular coupling when Cx43 proteins levels were decreased by ~40%, comparable to the level of reduction that we found in HF rabbit LV.⁴ We then went on to perform important complementary studies where we overexpressed wild-type Cx43 in isolated myocytes from our arrhythmogenic rabbit model of non-ischaemic HF. By using an adenovirus encoding a wild-type Cx43 gene sequence, we found that 87% overexpression of Cx43 in isolated HF myocytes (about a 23% higher in Cx43 levels compared with control) resulted in a marked improvement in dye coupling compared with AdLacZ infected HF myocytes. One could argue that in the setting of increased total amount of Cx43 proteins, potential differences in phosphorylation status and distribution of overexpressed Cx43 proteins could affect intercellular coupling. Therefore, we assessed the distribution pattern and phosphorylation state of Cx43 proteins in Cx43 overexpressed HF myocytes and found that the distribution of Cx43 proteins and the ratio of non-phosphorylated Cx43 to phosphorylated Cx43 were similar to that in AdLacZ infected HF myocytes. As such, our current results further confirm that reduction of Cx43 protein expression to levels seen in HF is associated with reduced intercellular coupling. We believe that downregulation and dephosphorylation of Cx43 in HF are double insults that contribute to decreased coupling and ultimately arrhythmogenesis and sudden death; we cannot rule out that other factors may also be contributing.

We assessed the function of Cx43 protein in isolated rabbit myocytes *in vitro* using a dye coupling approach, as we did in our prior studies.⁴ It has been shown that dye permeability of gap junction channels can be connexin-specific and dye-selective (size and charge dependent).²⁶ Studies suggest that Cx43 has more pronounced dye transfer associated with a higher gap junction conductance (G_j) compared with other cardiac connexins (Cx40 and Cx45) and that Cx43 exhibits a higher selectivity to the anionic dye, LY.^{27,28} Concordant changes in electrical coupling and dye coupling have been found in most studies with Cx43.^{24,29–31} For example, concordant decreases were found in

neonatal rat ventricular myocytes that were overexpressing a Cx43 mutant²⁴ or that were infected with *Trypanosoma cruzi*, the parasitic cause of Chagas disease.²⁹ Concordant increase in dye transfer and G_j were noted in HeLa cells expressing Cx43 and Cx45 (but not Cx40) treated with AAP10 (anti-arrhythmic peptide 10).³⁰ To our knowledge, there have been no direct comparisons of τ to G_j (the technique that we use has only been used by a few groups), but Dong *et al.*³¹ showed a linear relationship between the rate constant of LY dye transfer and G_j in HeLa cells transfected with Cx43.

It has also been shown that redistribution of Cx43 can alter intercellular coupling in diseased heart.⁵ Cx43 lateralization was found in human infarct border zone myocytes from patients with compensated hypertrophy due to valvular aortic stenosis and in the dog heart with pacing-induced HF,^{5,6} and Cx43 remodelling has been associated with reduced longitudinal conduction velocity in hypertrophied right ventricle.³² N-cadherin, an anchoring protein, has been shown to co-localize with Cx43, and downregulation of N-cadherin could lead to slowing of conduction.³³ In the present study, we did not find enhanced lateralization of Cx43 proteins in LV tissue sections from our HF rabbit model, but we found a reduced total amount of Cx43 proteins co-localized with an unchanged distribution and expression of N-cadherin. Our findings are consistent with results from another non-ischaemic HF rabbit model (pacing-induced HF),³⁴ although they do not agree with those from pacing-induced HF dogs.⁶ Although we cannot exclude effects of our interventions on other Cx43-related proteins, our studies of knocking down Cx43 levels in control myocytes combined with studies of Cx43 over-expression in HF myocytes provide complementary support for the important contribution of Cx43 levels to intercellular coupling.

4.4 Implications

Our current results provide important evidence that, in addition to enhanced Cx43 dephosphorylation, downregulation of Cx43 contributes to decreased intercellular coupling in HF. Modulation of Cx43 could be a novel therapeutic approach to improve conduction and reduce the incidence of sudden cardiac death in HF patients.

Supplementary material

Supplementary material is available at *Cardiovascular Research* online.

Acknowledgements

The authors want to thank Dr Eric Beyer (University of Chicago, IL, USA) for providing the AdCx43WT and AdLacZ viruses.

Conflict of interest: none declared.

Funding

This research was supported in part by HL080093.

References

1. Packer M. Sudden unexpected death in patients with congestive heart failure: a second frontier. *Circulation* 1985;**72**:681–685.

2. Pogwizd SM. Nonreentrant mechanisms underlying spontaneous ventricular arrhythmias in a model of nonischemic heart failure in rabbits. *Circulation* 1995; **92**:1034–1048.
3. Anderson KP, Walker R, Urie P, Ershler PR, Lux RL, Karwande SV. Myocardial electrical propagation in patients with idiopathic dilated cardiomyopathy. *J Clin Invest* 1993; **92**:122–140.
4. Ai X, Pogwizd SM. Connexin 43 downregulation and dephosphorylation in nonischemic heart failure is associated with enhanced colocalized protein phosphatase type 2A. *Circ Res* 2005; **96**:54–63.
5. Kostin S, Rieger M, Dammer S, Hein S, Richter M, Klovekorn WP et al. Gap junction remodeling and altered connexin43 expression in the failing human heart. *Mol Cell Biochem* 2003; **242**:135–144.
6. Akar FG, Nass RD, Hahn S, Cingolani E, Shah M, Hesketh GG et al. Dynamic changes in conduction velocity and gap junction properties during development of pacing-induced heart failure. *Am J Physiol Heart Circ Physiol* 2007; **293**:H1223–H1230.
7. Bastiaanse EM, Jongsma HJ, van der Laarse A, Takens-Kwak BR. Heptanol-induced decrease in cardiac gap junctional conductance is mediated by a decrease in the fluidity of membranous cholesterol-rich domains. *J Membr Biol* 1993; **136**:135–145.
8. Nelson WL, Makielski JC. Block of sodium current by heptanol in voltage-clamped canine cardiac Purkinje cells. *Circ Res* 1991; **68**:977–983.
9. Pappas CA, Rioult MG, Ransom BR. Octanol, a gap junction uncoupling agent, changes intracellular [H⁺] in rat astrocytes. *Glia* 1996; **16**:7–15.
10. Guerrero PA, Schuessler RB, Davis LM, Beyer EC, Johnson CM, Yamada KA et al. Slow ventricular conduction in mice heterozygous for a connexin43 null mutation. *J Clin Invest* 1997; **99**:1991–1998.
11. Eloff BC, Lerner DL, Yamada KA, Schuessler RB, Saffitz JE, Rosenbaum DS. High resolution optical mapping reveals conduction slowing in connexin43 deficient mice. *Cardiovasc Res* 2001; **51**:681–690.
12. Morley GE, Vaidya D, Samie FH, Lo C, Delmar M, Jalife J. Characterization of conduction in the ventricles of normal and heterozygous Cx43 knockout mice using optical mapping. *J Cardiovasc Electrophysiol* 1999; **10**:1361–1375.
13. Danik SB, Liu F, Zhang J, Suk HJ, Morley GE, Fishman GI et al. Modulation of cardiac gap junction expression and arrhythmic susceptibility. *Circ Res* 2004; **95**:1035–1041.
14. Kwak BR, Jongsma HJ. Regulation of cardiac gap junction channel permeability and conductance by several phosphorylating conditions. *Mol Cell Biochem* 1996; **157**:93–99.
15. Polontchouk LO, Valiunas V, Haefliger JA, Eppenberger HM, Weingart R. Expression and regulation of connexins in cultured ventricular myocytes isolated from adult rat hearts. *Pflugers Arch* 2002; **443**:676–689.
16. Berger HJ, Prasad SK, Davidoff AJ, Pimental D, Ellingsen O, Marsh JD et al. Continual electric field stimulation preserves contractile function of adult ventricular myocytes in primary culture. *Am J Physiol* 1994; **266**:H341–H349.
17. Eckardt D, Theis M, Degen J, Ott T, van Rijen HV, Kirchhoff S et al. Functional role of connexin43 gap junction channels in adult mouse heart assessed by inducible gene deletion. *J Mol Cell Cardiol* 2004; **36**:101–110.
18. Gutstein DE, Morley GE, Tamaddon H, Vaidya D, Schneider MD, Chen J et al. Conduction slowing and sudden arrhythmic death in mice with cardiac-restricted inactivation of connexin43. *Circ Res* 2001; **88**:333–339.
19. Pattison JS, Waggoner JR, James J, Martin L, Gulick J, Osinska H et al. Phospholamban overexpression in transgenic rabbits. *Transgenic Res* 2008; **17**:157–170.
20. Nishizawa T, Vatner SF, Hong C, Shen YT, Hardt SE, Robbins J et al. Overexpressed cardiac G α in rabbits. *J Mol Cell Cardiol* 2006; **41**:44–50.
21. Bers DM. Control of cardiac contraction by SR and sarcolemmal Ca Fluxes. *Excitation–Contraction Coupling and Cardiac Contractile Force*. 2nd ed. Kluwer Academic Publishers; 2001. p250.
22. Wang X, Gerdes AM. Chronic pressure overload cardiac hypertrophy and failure in guinea pigs: III. Intercalated disc remodeling. *J Mol Cell Cardiol* 1999; **31**:333–343.
23. Roell W, Lewalter T, Sasse P, Tallini YN, Choi BR, Breitbach M et al. Engraftment of connexin 43-expressing cells prevents post-infarct arrhythmia. *Nature* 2007; **450**:819–824.
24. Kizana E, Chang CY, Cingolani E, Ramirez-Correa GA, Sekar RB, Abraham MR et al. Gene transfer of connexin43 mutants attenuates coupling in cardiomyocytes: novel basis for modulation of cardiac conduction by gene therapy. *Circ Res* 2007; **100**:1597–1604.
25. Yao JA, Gutstein DE, Liu F, Fishman GI, Wit AL. Cell coupling between ventricular myocyte pairs from connexin43-deficient murine hearts. *Circ Res* 2003; **93**:736–743.
26. Abbaci M, Barberi-Heyob M, Blondel W, Guillemin F, Didelon J. Advantages and limitations of commonly used methods to assay the molecular permeability of gap junctional intercellular communication. *Biotechniques* 2008; **45**:33–52. 56–62.
27. Valiunas V, Beyer EC, Brink PR. Cardiac gap junction channels show quantitative differences in selectivity. *Circ Res* 2002; **91**:104–111.
28. Veenstra RD, Wang HZ, Beblo DA, Chilton MG, Harris AL, Beyer EC et al. Selectivity of connexin-specific gap junctions does not correlate with channel conductance. *Circ Res* 1995; **77**:1156–1165.
29. de Carvalho AC, Tanowitz HB, Wittner M, Dermietzel R, Roy C, Hertzberg EL et al. Gap junction distribution is altered between cardiac myocytes infected with *Trypanosoma cruzi*. *Circ Res* 1992; **70**:733–742.
30. Hagen A, Dietze A, Dhein S. Human cardiac gap-junction coupling: effects of anti-arrhythmic peptide AAP10. *Cardiovasc Res* 2009; **83**:405–415.
31. Dong L, Liu X, Li H, Vertel BM, Ebihara L. Role of the N-terminus in permeability of chicken connexin45.6 gap junctional channels. *J Physiol* 2006; **576**:787–799.
32. Uzzaman M, Honjo H, Takagishi Y, Emdad L, Magee AI, Severs NJ et al. Remodeling of gap junctional coupling in hypertrophied right ventricles of rats with monocrotaline-induced pulmonary hypertension. *Circ Res* 2000; **86**:871–878.
33. Li J, Patel VV, Kostetskii I, Xiong Y, Chu AF, Jacobson JT et al. Cardiac-specific loss of N-cadherin leads to alteration in connexins with conduction slowing and arrhythmogenesis. *Circ Res* 2005; **97**:474–481.
34. Wiegerinck RF, van Veen TA, Belterman CN, Schumacher CA, Noorman M, de Bakker JM et al. Transmural dispersion of refractoriness and conduction velocity is associated with heterogeneously reduced connexin43 in a rabbit model of heart failure. *Heart Rhythm* 2008; **5**:1178–1185.